

Affinity, Kinetic, and Structural Study of the Interaction of 3-*O*-Sulfotransferase Isoform 1 with Heparan Sulfate[†]

Eva Muñoz,[‡] Ding Xu,[§] Melissa Kemp,[‡] Fuming Zhang,[‡] Jian Liu,[§] and Robert J. Linhardt^{*;‡}

Departments of Chemistry and Chemical Biology, Biology, and Chemical and Biological Engineering, Rensselaer Polytechnic Institute, Troy, New York 12180, and Department of Medicinal Chemistry, University of North Carolina, Chapel Hill, North Carolina 27599

Received November 23, 2005; Revised Manuscript Received March 7, 2006

ABSTRACT: The 3-*O*-sulfonation of glucosamine residues in heparan sulfate (HS) by 3-*O*-sulfotransferase (3-OST) is a key substitution that is present in HS sequences of biological importance, in particular HS anticoagulant activity. Six different isoforms of 3-OST have been identified that exhibit different substrate specificity. In this paper the affinity and kinetics of the interaction between 3-*O*-sulfotransferase isoform 1 (3-OST-1) and HS have been examined using surface plasmon resonance (SPR). 3-OST-1 binds with micromolar affinity to HS ($K_D = 2.79 \mu\text{M}$), and this interaction is apparently independent of the presence of the coenzyme, 3'-phosphoadenosine 5'-phosphosulfate (PAPS). A conformational change in the complex has also been detected, supporting data from previous studies. Selected 3-OST-1 mutants have provided valuable information of amino acid residues that participate in 3-OST-1 interaction with HS substrate and its catalytic activity. The results from this study contribute to understanding the substrate specificity among the 3-OST isoforms and in the mechanism of 3-OST-1-catalyzed biosynthesis of anticoagulant HS.

Heparan sulfate proteoglycans (HSPGs)¹ are protein–carbohydrate conjugates present in the extracellular matrix and surface of most mammalian cells. HSPGs participate in a diverse number of biological processes including blood coagulation, viral infection, cell growth and development, tumor metastasis, and angiogenesis (1–5). They are comprised of one or more heparan sulfate (HS) glycosaminoglycan chains covalently attached to a core protein (1, 6). These HS chains bind to numerous proteins and are, thus, responsible for most of the biological functions of HSPGs (7, 8). HS are highly sulfated, linear polysaccharides comprised of a repeating disaccharide unit of sulfated β -D-glucuronic/ α -L-iduronic acid 1→4-linked to α -D-glucosamine residues. Sulfo groups can be present in the 2-*O*-position of the uronic acid and the 2-*N*-, 6-*O*-, and 3-*O*-positions of the glucosamine residues. Structural variations in HS lead to the presence of specific and often rare saccharide sequences within HS that determine the specificity and protein binding properties of HS (8). HS is initially synthesized in the Golgi as a copolymer of glucuronic acid and *N*-acetylglucosamine attached to a linkage region within its core protein. Subsequent structural modifications are achieved through the action

of a series of biosynthetic enzymes that are believed to act in a sequential manner. The *N*-deacetylase *N*-sulfotransferase catalyzes *N*-deacetylation/*N*-sulfation of glucosamine residues. The C₅ epimerase converts glucuronic acid into iduronic acid followed by *O*-sulfonation of the 2-*O*-position of the uronic acid and the 6-*O*- and 3-*O*-positions of the glucosamine unit, catalyzed by 2-OST, 6-OST, and 3-OST, respectively (9). The actions of these biosynthetic steps are often incomplete, resulting in a large number of permutations in the sequence of HS.

Sulfotransferases transfer the sulfuryl group from the donor PAPS to specific positions of the uronic acid and glucosamine residues (Figure 1A). While there is only a single 2-OST, there are two isoforms of 6-OST and seven isoforms of 3-OST (10). The large number of 3-OST isoforms is of particular interest since 3-*O*-sulfonation represents the final modification step in HS biosynthesis. Moreover, while the 3-*O*-sulfo group is only infrequently present in HS, it is a key substitution in important biological processes involved in blood anticoagulation, HSV infection, regulation of circadian rhythms, and various human cancers (11–13). The seven different 3-OST isoforms are believed to exhibit both tissue expression patterns (14) and different substrate specificity (15, 16). As a consequence, different isoforms are involved in the biosynthesis of different 3-*O*-sulfo groups containing HS sequences that can exhibit specific biological functions. The 3-OST-1 and 3-OST-5 isoforms are involved in the biosynthesis of the pentasaccharide sequence within HS that binds antithrombin (14, 17–19). The 3-OST-3, 3-OST-5, and 3-OST-6 generate a critical 3-*O*-sulfo group present in the HS sequence that binds HSV-1 glycoprotein gD (10, 12, 17, 20). Thus, the biosynthesis of specific 3-*O*-sulfo groups containing HS sequences is presumably regu-

[†] This work is supported in part by NIH Grants HL52622, HL62244, and GM38060 (to R.J.L.) and AI 50050 (to J.L.). D.X. is a recipient of a predoctoral fellowship from the American Heart Association MidAtlantic Affiliate.

* To whom correspondence should be addressed. Phone: (518) 276-3404. Fax: (518) 276-3405. E-mail: linhar@rpi.edu.

[‡] Rensselaer Polytechnic Institute.

[§] University of North Carolina.

¹ Abbreviations: HSPGs, heparan sulfate proteoglycans; HS, heparan sulfate; PAPS, 3'-phosphoadenosine 5'-phosphosulfate; HSV, herpes simplex virus; 3-OST, 3-*O*-sulfotransferase; PAP, 3'-phosphoadenosine 5'-phosphate; SPR, surface plasmon resonance; SA, streptavidin; FC, flow cell; ITC, isothermal titration calorimetry.

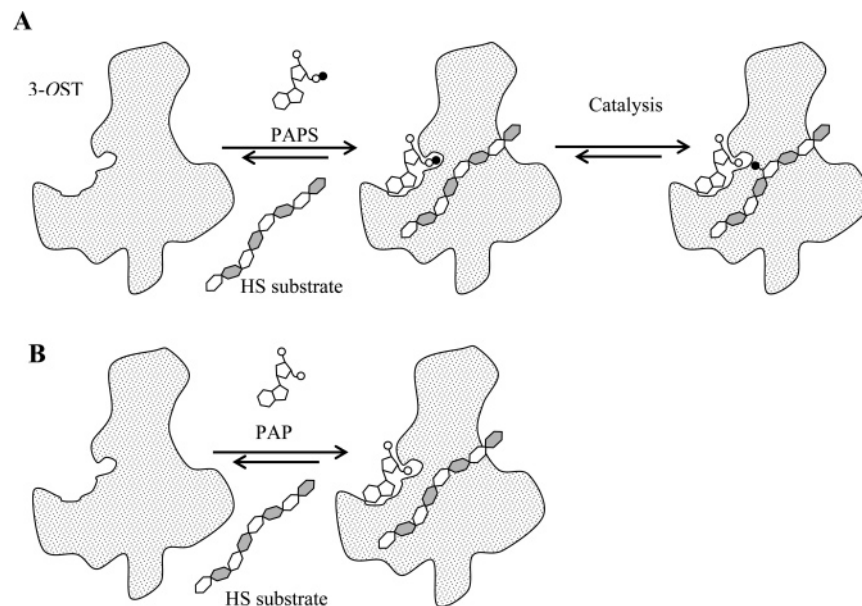


FIGURE 1: (A) Schematic of 3-*O*-sulfonation of HS by 3-OST-1. After formation of the ternary complex PAPS–3-OST–HS the enzyme transfers the sufo group (●) from the sulfuryl donor PAPS to the HS polysaccharide substrate. (B) A ternary complex PAP–3-OST–HS is formed, but PAP lacks a sulfo group to transfer so no catalysis results.

lated by both the specificity of the cell and tissue expression of the 3-OST isoforms as well as by their defined substrate specificities. The mechanism that underlies the specificity of the different 3-OST isoforms is unknown.

Over the past several years, studies from our laboratory and others have been published on 3-OST substrate specificity (19, 21–25). In these studies, some structural characteristics of the HS oligosaccharides that are selectively recognized by 3-OST-1, 3-OST-3, and 3-OST-5 have been elucidated. We have recently reported the crystal structure of 3-OST-3 in a ternary complex of a tetrasaccharide substrate and PAP (Figure 1B), the product formed after sulfuryl transfer takes places from PAPS (26). This work afforded structural information at the atomic level of the ternary complex and provided new insights into HS substrate recognition. This structural information, together with the crystal structure of 3-OST-1 in a binary complex with PAP (27), is being used to develop an improved understanding of the mechanism of action of the entire 3-OST family through structure-based homology modeling studies (28). On the basis of these studies, the PAP and HS substrate binding sites in 3-OST-1 were predicted and a number of amino acid residues relevant for the enzymatic process were proposed, and site-directed mutagenesis revealed residues that were important for the binding of the enzyme to PAPS. As part of our continuing study, we report HS binding analysis of the wild-type 3-OST-1 and selected 3-OST-1 mutants using SPR. This study provides valuable information on amino acid residues that are involved in HS substrate binding and the catalytic mechanism of 3-OSTs.

EXPERIMENTAL PROCEDURES

Materials

[³⁵S]PAPS was prepared by incubating 0.4–2 mCi/mL [³⁵S]Na₂SO₄ (carrier-free, MP Biomedical) and 16 mM ATP with 5 mg/mL dialyzed yeast extract (Sigma), following a

protocol described by Bame and Esko (29). HS from bovine kidney was purified in our laboratory. PAP was purchased from Sigma. Porcine intestinal heparan sulfate (14.8 kDa) and dermatan sulfate (30 kDa) were from Celsus (Cincinnati, OH). Chondroitin sulfate A (20 kDa, bovine trachea), chondroitin sulfate C (20 kDa, shark cartilage), hyaluronic acid (100 kDa, *Streptococcus zooepidemicus*), and Triton X-100 were from Sigma (St. Louis, MO). Sulfo-*N*-hydroxy-succinimide long-chain biotin was from Pierce (Rockford, IL). Streptavidin (SA) sensor chips, sodium acetate (pH = 4.5), and HBS-EP buffer (0.01 M HEPES, pH = 7.4, 0.15 M NaCl, 3 mM EDTA, 0.005% surfactant P20) were from BIAcore (Biacore AB, Uppsala, Sweden). Phosphate running buffer (0.1 M sodium phosphate, pH = 7.0, 0.1 M NaCl, 0.1% Triton X-100) was prepared from monobasic and dibasic phosphate (Mallinckrodt) and doubly distilled water. All of the buffers were filtered (0.22 μm) and degassed prior to use. SPR measurements were performed on a BIAcore 3000 instrument with BIAcore 3000 control and BIAevaluation software (version 4.0.1).

Methods

Expression and Purification of Wild-Type 3-OST-1 and 3-OST-1 Mutants. The preparations of the expression plasmids are described elsewhere (27). Expression of wild-type mouse 3-OST-1 and 3-OST-1 mutants was carried out in Rosetta 2 cells (Novagen). Briefly, Rosetta 2 cells containing the 3-OST-1-pET28 were grown in LB media with 15 μg/mL kanamycin and 35 μg/mL chloramphenicol at 37 °C. When the A₆₀₀ reached 0.6–0.8, IPTG was then added to a final concentration of 0.2 mM, and the cells were allowed to shake overnight at 22 °C. Cells were pelleted and resuspended in the sonication buffer containing 25 mM Tris, pH 7.5, 500 mM NaCl, and 20 mM imidazole. Cells were disrupted by sonication and then spun down. The supernatant was applied to a Ni–Sepharose 6 fast-flow column (1 × 10 cm; Amersham) and washed with the sonication buffer. The

bound protein was eluted with an imidazole gradient from 20 to 250 mM in 100 mL at a flow rate of 4 mL/min. The purified protein migrated at 33 kDa on 12% SDS-PAGE with the purity greater than 95%. The concentration of the protein was determined by the BCA kit (Sigma). The specific enzymatic activity of wild-type 3-OST-1 was determined to be 14 pmol of sulfate/ μ g.

Because the 3-OST-1 mutants are catalytically inactive proteins, it is not possible to follow the enzymatic activity as described below during the purification. The procedure for the expression and purification of these mutant proteins followed the identical one that was used for the wild-type protein. The migration profiles of the purified mutants were identical to that of wild-type 3-OST-1 on SDS-PAGE and showed greater than 95% purity. The specific activity of 3-OST-1 E90Q and 3-OST-1 R276A is less than 0.14 pmol/ μ g.

Determination of the Activity of the Wild-Type 3-OST-1. Recombinant wild-type 3-OST-1 (0.5 μ g) was mixed with 1 μ g of HS (from bovine kidney) in a buffer containing [35 S]-PAPS (1×10^6 cpm), 50 mM MES, 10 mM MnCl₂, 5 mM MgCl₂, and 1% Triton X-100 (pH 7) and 0.1 mg/mL bovine serum albumin. The reaction was incubated at 37 °C for 1 h and was then subjected to a 200 μ L DEAE-Sepharose column (0.5 \times 1 cm) to purify [35 S]HS (30). The amount of [35 S]HS was proportional to the concentration of 3-OST-1 in the reaction. Wild-type 3-OST-1 (10 μ g) typically affords 2.8×10^6 cpm of [35 S]HS, which is about 1000-fold above the background. The "inactive" mutants used in this study have 1% or less of the wild-type activity.

Preparation of the HS Sensor Chip. HS was attached to the SA sensor chip surface by noncovalent capture of biotin to streptavidin. The biotinylated HS was prepared by reaction of sulfo-*N*-hydroxysuccinimide long-chain biotin with free amino groups of unsubstituted glucosamine residues in the polysaccharide chain following a published procedure (30). A solution of the HS-biotin conjugate (0.1 mg/mL) in HBS-EP running buffer was injected over flow cell 2 (FC2) or FC4 of the SA chip at a flow rate of 5 μ L/min and 25 °C. A manual injection mode was used, and the immobilization of the ligand to the surface was monitored as a function of time (sensorgram). HS surfaces were created with 1390 and 479 RU immobilization levels in FC2 and FC4, respectively. FC1 and FC3, without HS, served as control.

Binding Study of the Interaction of Wild-Type 3-OST-1 and 3-OST-1 Mutants with HS. A solution of the protein (950 nM) in phosphate running buffer was injected over FC1 (control) and FC2 (1390 RU in HS) of the SA sensor chip (flow rate = 40 μ L/min, $T = 25$ °C). A kinetic injection mode was used, flowing the protein for 3 min and monitoring the dissociation for another 3 min. The response was monitored as a function of time, and after each analyte injection the surface was regenerated with 1 min injection of 2 M NaCl followed by 1 min injection of sodium acetate (pH = 4.5). The response in FC1 was subtracted from the response in FC2, and the resulting sensorgrams were analyzed with BIAevaluation software.

Affinity and Kinetic Analysis of the Interaction of Wild-Type 3-OST-1 and 3-OST-1-PAP E90Q and R276A Mutants with HS. Wild-type 3-OST-1, E90Q, or R276A was injected at different concentrations (250, 500, 750, 950, 1500, and 2000 nM) in phosphate running buffer over FC3 (control)

and FC4 (479 RU in HS) of the SA sensor chip (flow rate = 40 μ L/min, 25 °C). For the interaction of 3-OST-1-PAP with HS, phosphate running buffer containing PAP (40 μ M) was used to prepare the analyte solutions. A kinetic injection mode was used, flowing the protein for 3 min and monitoring the dissociation for another 3 min. The response was monitored as a function of time, and after each analyte injection the surface was regenerated with 1 min injection of 2 M NaCl followed by 1 min injection of sodium acetate (pH = 4.5). The response in FC3 was subtracted from the response in FC4, and the resulting sensorgrams were analyzed with BIAevaluation software.

Variable Contact Time Experiment of the Interaction of 3-OST-1 with HS. A solution of 3-OST-1 (950 nM) in phosphate running buffer was injected at different injection times (30, 60, 120, 180, and 300 s) over FC1 (control) and FC2 (1390 RU in HS) of the SA sensor chip. A kinetic injection mode was used, flowing the protein for 30, 60, 120, 180, or 300 s and monitoring the dissociation for 3 min. The response was monitored as a function of time, and after each analyte injection the surface was regenerated with 1 min injection of 2 M NaCl followed by 1 min injection of sodium acetate (pH = 4.5). The conformational change that occurs in the complex was examined by comparison of the dissociation phase of the normalized sensorgrams. The response in FC1 was subtracted from the response in FC2, and the resulting sensorgrams were analyzed with BIAevaluation software.

Solution Competition SPR Study. To perform solution competition SPR studies, 3-OST-1 (500 nM) was premixed with different concentrations of heparin (1 nM–1 μ M), HS (10 nM–10 μ M), dermatan sulfate, chondroitin sulfate A, and chondroitin sulfate C (500 nM–10 μ M), and hyaluronic acid (500 nM–1 μ M) in phosphate running buffer and injected over a HS chip (flow rate of 40 μ L/min, 25 °C). A kinetic injection mode was used to monitor the association for 3 min and the dissociation for another 3 min. The surface was regenerated with consecutive 1 min injections of 50 mM NaOH, 1 M NaCl, and 2 M NaCl. For each set of glycosaminoglycans a control injection, with only 3-OST-1, was performed to ensure the surface remained active. The maximum response units were used for the IC₅₀ calculation (31).

RESULTS

SPR Affinity and Kinetic Analysis of the Interaction of 3-OST-1 with HS. The binding between 3-OST-1 and HS was examined by SPR. Biotinylated HS was immobilized to a SA sensor chip (FC4, 479 RU), and the enzyme in phosphate running buffer was injected at different concentrations (250–2000 nM) over the HS surface. The response obtained in the control flow cell (FC3) represented less than 5% of the overall response from the interaction of 3-OST-1 with HS in FC4. Attempts to fit the sensorgrams to a simple 1:1 Langmuir binding equation failed. A good fit of the experimental data was achieved only when a two-state reaction model was used (Figure 2A). This model considers a 1:1 binding of the analyte to the immobilized ligand followed by a conformational change in the complex. The two-state reaction model is described in eq 1, where k_{on} and k_{off} are the on and off rate constants of the binding process

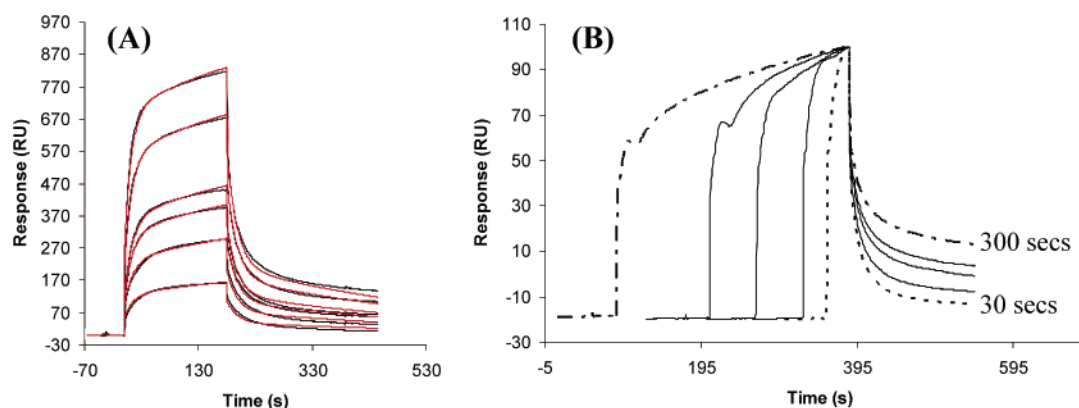


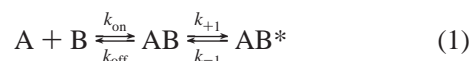
FIGURE 2: (A) Sensorgrams of the interaction of 3-OST-1 (250, 500, 750, 950, 1500, and 2000 nM) with HS. Global fitting of the sensorgrams to a two-state reaction model (curves in red) was achieved. (B) Sensorgrams of the interaction between 3-OST-1 and HS using different injection times (30, 60, 90, 180, and 300 s). For a better comparison the curves have been normalized and aligned to the end point of the injection.

Table 1: SPR Affinity and Kinetic Data of the Interaction of 3-OST-1, 3-OST-1-PAP, R276A, and E90Q with HS

	$k_{on}^a (\times 10^4 \text{ M}^{-1} \text{ s}^{-1})$	$k_{off}^a (\times 10^{-2} \text{ s}^{-1})$	$K_{+1}^b (\times 10^{-3} \text{ s}^{-1})$	$K_{-1}^b (\times 10^{-3} \text{ s}^{-1})$	$K_D (\mu\text{M})$	χ^2
3-OST-1 vs HS	1.46 ± 0.02	5.40 ± 0.07	3.20 ± 0.03	2.41 ± 0.04	2.79	52.5
3-OST-1-PAP vs HS	1.31 ± 0.05	6.0 ± 0.2	4.9 ± 0.1	4.7 ± 0.5	4.4	4.7
R276A vs HS	1.1 ± 0.4	15 ± 3	6 ± 2	2.64 ± 0.01	7	
E90Q vs HS	15 ± 2	38 ± 5	2.5 ± 0.6	2.3 ± 0.2	2.5	

^a K_{on} , K_{off} : on and off rate constants of the binding step. ^b K_{+1} , K_{-1} : on and off rate constants of the conformational change.

between ligand and analyte and k_{+1} and k_{-1} are the rate constants of the conformational change.



The overall dissociation constant (K_D) is calculated as $K_D = (k_{off}/k_{on})(k_{-1}/k_{+1})$. Global fitting of the sensorgrams provided on and off rate constants of the binding and the conformational change equilibrium from which a K_D of 2.79 μM was calculated (Table 1).

Additional information of the conformational change was achieved with an experiment that varied the contact time between ligand and analyte. In this experiment, 3-OST-1 (950 nM) in phosphate running buffer was injected over the HS surface at different injection times (30, 60, 90, 180, and 300 s). Longer dissociation times allow the conformational change to take place in a greater extent, generating a more stable conformation, and is reflected in a slower dissociation rate. The resulting sensorgrams were normalized, and the dissociation phase of each was compared. The interaction between 3-OST-1 and HS shows a slower dissociation phase when longer association times are used (Figure 2B). These results are consistent with a conformational change in 3-OST-1 occurring after binding to HS.

The binding of 3-OST-1 with HS was also investigated in the presence of PAP. PAP is the product formed when PAPS transfers its sulfuryl group. PAP has a similar affinity to 3-OST-1 as PAPS and is chemically more stable than PAPS (32). The dissociation constant of PAP with wild-type 3-OST-1 has been determined by isothermal titration calorimetry (ITC) to be $14 \pm 4 \mu\text{M}$ (27). This value is similar to the K_m value of 10 μM for PAPS with 3-OST-1 (33), suggesting that the PAP represents a good model for PAPS in studying the binding affinity to 3-OST-1. To measure the interaction of the binary complex 3-OST-1-PAP with HS,

3-OST-1 in phosphate running buffer containing an excess amount of PAP (40 μM) was injected over an HS sensor chip (FC4) at different concentrations (250–2000 nM). The sensorgrams were very similar to the sensorgrams observed for the interaction between 3-OST-1 and HS in the absence of PAP, and global fitting of the curves to a two-state reaction model gave comparable binding information (Table 1). This experiment suggests that the binding of 3-OST-1 to the HS substrate is independent of the interaction between 3-OST-1 and PAPS.

Selectivity of 3-OST-1 for Substrate Binding. Solution competition studies for 3-OST-1 interaction with various glycosaminoglycans were next undertaken. In phosphate running buffer 3-OST-1 was mixed with a range of glycosaminoglycan concentrations, flowed over a HS chip, and the IC_{50} for each interaction was estimated (31). Both HS and heparin are 3-OST-1 substrates. Soluble HS competed well with immobilized HS, giving an IC_{50} of $\sim 1 \mu\text{M}$, but heparin bound considerably more tightly with an IC_{50} of ~ 10 nM. Both chondroitin sulfate A and dermatan sulfate showed less binding avidity ($IC_{50} \sim 10 \mu\text{M}$) than either of the 3-OST-1 substrates. Neither chondroitin sulfate C nor hyaluronic acid interacted with 3-OST-1 over the range of concentrations examined. Finally, chondroitin sulfate C, dermatan sulfate, and hyaluronic acid (0.5 mg/mL) failed to inhibit 3-OST-1-catalyzed sulfonation of HS in enzyme assays, whereas chondroitin sulfate A (0.5 mg/mL) inhibits 15% of 3-OST-1 activity.

SPR Binding Analysis of the Interaction of Wild-Type 3-OST-1 and 3-OST-1 Mutants with HS. The crystal structure of 3-OST-1 in a binary complex with PAP has been reported (27). In this work a careful analysis of the 3-OST-1-PAP complex was carried out, and a prediction of residues that are involved in the enzymatic activity was proposed (27). On the basis of this analysis a total of 18 point mutants of

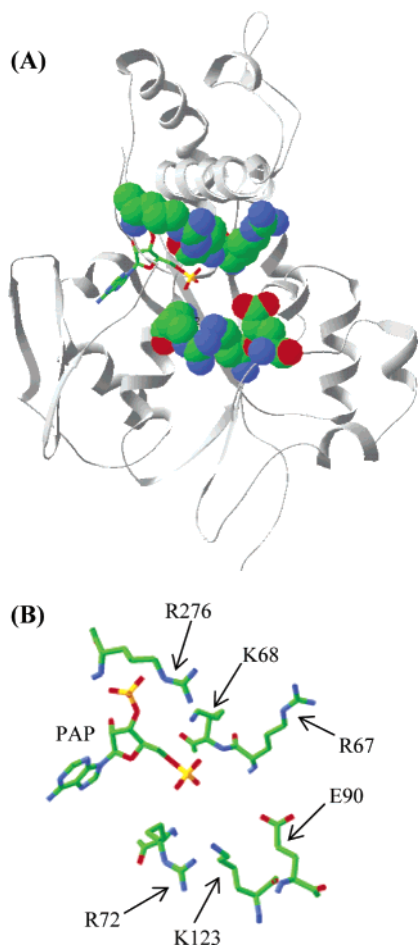


FIGURE 3: (A) Ribbon diagram of the crystal structure of the binary complex 3-OST-PAP. The amino acids that have been mutated for the structural analysis of the 3-OST-1-PAP interaction are highlighted (CPK). (B) PAP and amino acid residues mutated. The figure shows the relative position of the amino acids with respect to the PAP coenzyme.

3-OST-1 were prepared, and the enzymatic activity of these mutants was examined. Several point mutations abolished or significantly reduced the enzymatic activity, suggesting that these amino acids participate in the catalytic reaction or in the binding to PAPS or HS. The elucidation of residues involved in the binding of 3-OST-1 to PAPS was carried out by isothermal titration calorimetry binding studies of selected 3-OST-1 mutants with PAP. To extend this work, we conducted HS binding studies on a select group of 3-OST-1 mutants using SPR to detect amino acid residues involved in the interaction between the enzyme and substrate. Six point mutants were selected with mutations in positions R72, R67, K68, E90, K123, and R276 of the wild-type protein. Previous activity assays demonstrated that these mutants lack enzymatic activity (27). R72, R67, K68, K123, and R276 are basic arginine/lysine residues located in a large open cleft of 3-OST-1 that is believed to be the HS binding site (Figure 3). These residues probably assist in the binding with HS, interacting with negatively charged sulfo or carboxyl groups on the substrate. In the mutants studied (R72E, R67A, K68A, K123A, and R276A) these basic residues were substituted with neutral or acidic amino acids. E90 has been proposed to be the catalytic base responsible for 3-OST-1 activity (27).

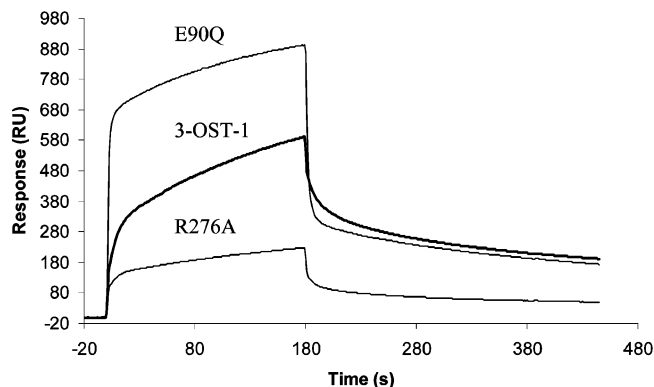


FIGURE 4: Sensorgrams of the interaction of 3-OST-1, R276A, and E90Q (950 nM) with HS.

The ability of the six 3-OST-1 mutants to bind HS was examined. A solution of the mutant (950 nM) in phosphate running buffer was injected over the HS sensor chip (FC2 and FC1 control). No response was observed when R72E, R67A, K68A, and K123A mutants were injected over the HS surface, demonstrating that these residues are essential for the binding of 3-OST-1 with HS. Mutants R276A and E90Q bound HS, but the resulting sensorgrams showed remarkable differences with the sensorgram of the interaction of the wild-type 3-OST-1 with HS (Figure 4). These data suggest that while amino acids R276 and E90 are not critical residues for the interaction of the enzyme with the substrate, these mutations influence the binding. A more detailed binding analysis of these mutants with HS was required to obtain further insight into the role of these residues in the 3-OST-1/HS interaction.

The binding affinity and kinetics of the interaction of the two mutants with HS were next carried out. R276A or E90Q 3-OST-1 mutant was injected at different concentrations (250–2000 nM) in phosphate running buffer over the HS sensor chip (FC4 and FC3 control). The best fit of the sensorgrams obtained was achieved when a two-state reaction model was used for both 3-OST-1 mutants. The affinity and kinetic constants of the interaction were obtained by individual fitting of the sensorgrams derived from different analyte concentrations. The final data are given as the average of the individual data accompanied by the standard error (Table 1). Global fitting of the sensorgrams yielded higher χ^2 values (data not shown).

R276A 3-OST-1 mutant binds HS with lower affinity ($K_D = 7.13 \mu\text{M}$) compared to the wild-type 3-OST-1 ($K_D = 2.79 \mu\text{M}$). Comparison of the rate constants derived from the fitting shows that the complex 3-OST-1 R276A mutant-HS dissociates faster ($k_{\text{off}} = 15.43 \times 10^{-2} \text{ s}^{-1}$) than the 3-OST-1-HS complex ($k_{\text{off}} = 5.96 \times 10^{-2} \text{ s}^{-1}$). These data demonstrate that the R276A residue is establishing a secondary interaction with HS that contributes to the stabilization of the enzyme-substrate complex; nevertheless, this secondary interaction is not essential for binding.

The 3-OST-1 E90Q mutant binds HS ($K_D = 2.51 \mu\text{M}$) with the same affinity as the wild-type 3-OST-1 ($K_D = 2.79 \mu\text{M}$), suggesting that E90 is not directly involved in the binding of 3-OST-1 with HS. The mutation does not affect the rate constants associated with the conformational change (k_{+1} and k_{-1}) but accelerates both on and off rate constants of the binding process by an order of magnitude (Table 1).

DISCUSSION

The 3-*O*-sulfonation of glucosamine residues in HS is a rare substitution that is present in HS oligosaccharide sequences of biological importance (34). The HS substrate used in this study contained no detectable 3-*O*-sulfo groups. Furthermore, monosaccharide analysis showed that the hexosamine component of this HS was 79% GlcNAc, 16% GlcNS, 4% GlcNAc6S, and 1% GlcNS6S and the uronic acid component was 72% GlcA, 27% IdoA, and 1% IdoA2S (35). The biosynthesis of the 3-*O*-sulfo group containing HS is a highly controlled biosynthetic step conducted by seven 3-OST isoforms that establish the structure of the HS product (10). An understanding of the substrate specificity of this reaction is important for the control of the biosynthesis of 3-*O*-sulfo group containing HS sequences having biologically significant activities. Both HS and heparin bind to 3-OST-1 and serve as substrates. Other glycosaminoglycans either fail to bind or bind less tightly than do these substrates. The PAPS coenzyme binding site is conserved among the sulfotransferases. However, the HS substrate binding site in 3-OST appears to contain structural variations that might alter its topology, serving as a tool for the selective recognition of specific HS substrates by different 3-OST isoforms. Thus, the elucidation of the binding and structural properties of the 3-OST-substrate complex is a key step for determining the mechanism of the substrate specificity among the 3-OST isoforms.

In this paper we present the affinity, kinetic, and structural study of the interaction between 3-OST-1 and HS. Using kinetic data of the substrate-enzyme interaction obtained by SPR, a dissociation constant of 2.79 μ M for the 3-OST-1-HS complex was calculated. The binding of 3-OST-1 to the substrate seems to be independent of the presence of the coenzyme (PAPS). A conformational change in 3-OST-1 takes place on complex formation. This observed conformational change is supported by previous studies that relied on fluorescence and chemical modification methods (27). To our knowledge, this is the first detailed affinity and kinetic study of the interaction of 3-OST-1 with HS.

The examination of the 3-OST-1 mutant interaction with HS provides structural information, revealing amino acid residues that are important for the binding of the enzyme to the HS substrate. The basic residues R72, R67, K123, and R276 are located in an open cleft that is proposed to be the HS binding site (Figure 3A). While site-directed mutagenesis of these residues abolishes the enzymatic activity, these 3-OST-1 mutants retain their ability to bind PAP (27). Single point mutations R72A, R67A, and K123A result in 3-OST-1 mutants that are inactive, probably as a result of their inability to bind HS substrate. Consequently, these amino acids form part of the HS binding site in 3-OST-1 that is essential for polysaccharide substrate binding. The R276A mutant binds HS but with lower affinity than wild-type 3-OST-1 (Table 1). This decrease in binding affinity is due to a faster dissociation of the enzyme from the HS substrate. These data demonstrate that R276 stabilizes the interaction of 3-OST-1 with HS, most probably through an electrostatic interaction with a sulfo group in the HS substrate. However, this interaction plays a secondary role and is not essential for the binding. Surprisingly, the R276A mutant lacks of enzymatic activity, suggesting that R276 participates in the

catalytic activity of the enzyme. This is supported by the proximity of R276 to PAP observed in the crystal structure of the 3-OST-1-PAP binary complex (Figure 3B). The K68A mutant partially retains PAP binding but has no enzymatic activity, suggesting that K68 is involved in the binding to PAPs; however, in the crystal structure of the 3-OST-1-PAP binary complex K68 is pointing outward toward the HS binding site (27) (Figure 3B). Binding studies on the K68A mutant 3-OST-1 with HS demonstrate markedly reduced substrate binding. The involvement of K68 in binding both PAP and HS suggests that this residue is involved in catalysis.

E90 is a conserved residue that is found on the inside of the large cleft and is proposed as the catalytic base for the activity of 3-OST-1. Mutation at E90 does not affect 3-OST-1 affinity for PAP (27) nor does it impact HS binding but instead results in a complete loss of enzymatic activity, supporting the current hypothesis that E90 is the catalytic base for 3-OST-1 activity.

In summary, we provide affinity and kinetic data of the interaction of 3-OST-1 with HS and additional proof of a conformational change that takes place on complex formation. This study provides valuable information with important implications for understanding the mechanism of the enzyme/substrate recognition and the catalytic activity of 3-OST-1. Comparison of the binding properties of the wild-type 3-OST-1 and selected mutants has identified amino acid residues critical in substrate binding and for catalytic activity, particularly E90, which we suggest is the catalytic base required for 3-OST-1 activity.

REFERENCES

- Rosenberg, R. D., Shworak, N. W., Liu, J., Schwartz, J. J., and Zhang, L. (1997) Heparan sulfate proteoglycans of the cardiovascular system. Specific structures emerge but how is synthesis regulated?, *J. Clin. Invest.* 100, S67-S75.
- Bernfield, M., Gotte, M., Park, P. W., Reizes, O., Fitzgerald, M. L., Lincoff, J., and Zako, M. (1999) Functions of cell surface heparan sulfate proteoglycans, *Annu. Rev. Biochem.* 68, 729-777.
- Liu, J., and Thorp, S. C. (2001) Cell surface heparan sulfate and its roles in assisting viral infections, *Med. Res. Rev.* 22, 1-25.
- Sasisekharan, R., Shriver, Z., Venkataraman, G., and Narayanasami, U. (2002) Roles of heparan-sulphate glycosaminoglycans in cancer, *Nat. Rev. Cancer* 2, 521-528.
- Moon, J. J., Matsumoto, M., Patel, S., Lee, L., Guan, J.-L., and Li, S. (2004) Role of cell surface heparan sulfate proteoglycans in endothelial cell migration and mechanotransduction, *J. Cell. Physiol.* 203, 166-176.
- Lindahl, U., Kusche-Gullberg, M., and Kjellen, L. (1998) Regulated diversity of heparan sulfate, *J. Biol. Chem.* 273, 24979-24982.
- Capila, I., and Linhardt, R. J. (2002) Heparin-protein interactions, *Angew. Chem., Int. Ed.* 41, 390-412.
- Coombe, D. R., and Kett, W. C. (2005) Heparan sulfate-protein interactions: therapeutic potential through structure-function insights, *Cell. Mol. Life Sci.* 62, 410-424.
- Sasisekharan, R., and Venkataraman, G. (2000) Heparin and heparan sulfate: biosynthesis, structure and function, *Curr. Opin. Chem. Biol.* 4, 626-631.
- Xu, D., Tiwari, V., Xia, G., Clement, C., Shukla, D., and Liu, J. (2005) Characterization of heparan sulphate 3-O-sulphotransferase isoform 6 and the role in assisting the entry of herpes simplex virus, type 1, *Biochem. J.* 385, 451-459.
- Liu, J., Shworak, N. W., Fritze, L. M., Edelberg, J. M., and Rosenberg, R. D. (1996) Purification of heparan sulfate D-glucosaminyl 3-O-sulphotransferase, *J. Biol. Chem.* 271, 27072-27082.

12. Shukla, D., Liu, J., Blaiklock, P., Shworak, N. W., Bai, X., Esko, J. D., Cohen, G. H., Eisenberg, R. J., Rosenberg, R. D., and Spear, P. G. (1999) A novel role for 3-O-sulfated heparan sulfate in herpes simplex virus 1 entry, *Cell* 99, 13–22.
13. Ye, S., Luo, Y., Lu, W., Jones, R. B., Linhardt, R. J., Capila, I., Toida, T., Kan, M., Pelletier, H., and McKeehan, W. L. (2001) Structural basis for interaction of FGF-1, FGF-2 and FGF-7 with different heparan sulfate motifs, *Biochemistry* 40, 14429–14439.
14. Shworak, N. W., Liu, J., Petros, L. M., Zhang, L., Kobayashi, M., Copeland, N. G., Jenkins, N. A., and Rosenberg, R. D. (1999) Multiple isoforms of heparan sulfate D-glucosaminyl 3-O-sulfotransferase. Isolation, characterization, and expression of human cdnas and identification of distinct genomic loci, *J. Biol. Chem.* 274, 5170–5184.
15. Liu, J., Shworak, N. W., Sinay, P., Schwartz, J. J., Zhang, L., Fritze, L. M. S., and Rosenberg, R. D. (1999) Expression of heparan sulfate D-glucosaminyl 3-O-sulfotransferase isoforms reveals novel substrate specificities, *J. Biol. Chem.* 274, 5185–5192.
16. Taniguchi, N., Honke, K., and Fukuda, M., Eds. (2002) *Handbook of Glycosyltransferases and Related Genes*, Springer-Verlag, New York.
17. Xia, G., Chen, J., Tiwari, V., Ju, W., Li, J.-P., Malmstrom, A., Shukla, D., and Liu, J. (2002) Heparan sulfate 3-O-sulfotransferase isoform 5 generates both an antithrombin-binding site and an entry receptor for herpes simplex virus-1, *J. Biol. Chem.* 277, 37912–37919.
18. Duncan, M. B., Chen, J., Krise, J. P., and Liu, J. (2004) The biosynthesis of anticoagulant heparan sulfate by the heparan sulfate 3-O-sulfotransferase isoform 5, *Biochim. Biophys. Acta* 1671, 34–43.
19. Chen, J., and Liu, J. (2005) Characterization of the structure of antithrombin-binding heparan sulfate generated by heparan sulfate 3-O-sulfotransferase 5, *Biochim. Biophys. Acta* 1725, 190–200.
20. Tiwari, V., Clement, C., Duncan, M. B., Chen, J., Liu, J., and Shukla, D. (2004) A role for 3-O-sulfated heparan sulfate in cell fusion induced by herpes simplex virus type 1, *J. Gen. Virol.* 85, 805–809.
21. Liu, J., Shworak, N. W., Sinay, P., Schwartz, J. J., Zhang, L., Fritze, L. M., and Rosenberg, R. D. (1999) Expression of heparan sulfate D-glucosaminyl 3-O-sulfotransferase isoforms reveals novel substrate specificities, *J. Biol. Chem.* 274, 5185–5192.
22. Liu, J., Shriver, Z., Blaiklock, P., Yoshida, K., Sasisekharan, R., and Rosenberg, R. D. (1999) Heparan sulfate D-glucosaminyl 3-O-sulfotransferase-3A sulfates N-unsubstituted glucosamine residues, *J. Biol. Chem.* 274, 38155–38162.
23. Zhang, L., Lawrence, R., Schwartz, J. J., Bai, X., Wei, G., Esko, J. D., and Rosenberg, R. D. (2001) The effect of precursor structures on the action of glucosaminyl 3-O-sulfotransferase-1 and the biosynthesis of anticoagulant heparan sulfate, *J. Biol. Chem.* 276, 28806–28813.
24. Liu, J., Shriver, Z., Pope, R. M., Thorp, S. C., Duncan, M. B., Copeland, R. J., Raska, C. S., Yoshida, K., Eisenberg, R. J., Cohen, G., Linhardt, R. J., and Sasisekharan, R. (2002) Characterization of a heparan sulfate octasaccharide that binds to herpes simplex virus type 1 glycoprotein D, *J. Biol. Chem.* 277, 33456–33467.
25. Chen, J., Duncan, M. B., Carrick, K., Pope, R. M., and Liu, J. (2003) Biosynthesis of 3-O-sulfated heparan sulfate: unique substrate specificity of heparan sulfate 3-O-sulfotransferase isoform 5, *Glycobiology* 13, 785–794.
26. Moon, A. F., Edavettal, S. C., Krahn, J. M., Munoz, E. M., Negishi, M., Linhardt, R. J., Liu, J., and Pedersen, L. C. (2004) Structural analysis of the sulfotransferase (3-O-sulfotransferase isoform 3) involved in the biosynthesis of an entry receptor of herpes simplex virus 1, *J. Biol. Chem.* 279, 45185–45193.
27. Edavettal, S. C., Lee, K. A., Negishi, M., Linhardt, R. J., Liu, J., and Pedersen, L. C. (2004) Crystal structure and mutational analysis of heparan sulfate 3-O-sulfotransferase isoform 1, *J. Biol. Chem.* 279, 25789–25797.
28. Raman, R., Myette, J., Venkataraman, G., Sasisekharan, V., and Sasisekharan, R. (2002) Identification of structural motifs and amino acids within the structure of human heparan sulfate 3-O-sulfotransferase that mediate enzymatic function, *Biochem. Biophys. Res. Commun.* 290, 1214–1219.
29. Bame, K. J., and Esko, J. D. (1989) Under sulfated heparan sulfate in a Chinese hamster ovary cell mutant defective in heparan sulfate N-sulfotransferase, *J. Biol. Chem.* 264, 8059–8065.
30. Hernaiz, M., Liu, J., Rosenberg, R. D., and Linhardt, R. J. (2000) Enzymatic modification of heparan sulfate on a biochip promotes its interaction with antithrombin III, *Biochem. Biophys. Res. Commun.* 276, 292–297.
31. Zhang, F., Ronca, F., Linhardt, R. J., and Margolis, R. U. (2004) Structural determinants of heparan sulfate interactions with Slit proteins, *Biochem. Biophys. Res. Commun.* 317, 352–357.
32. Negishi, M., Pedersen, L. G., Petrotchenko, E., Shevtsov, S., Gorokhov, A., Kakuta, Y., and Pedersen, L. C. (2001) Structure and function of sulfotransferases, *Arch. Biochem. Biophys.* 390, 149–157.
33. Myette, J. R., Shriver, Z., Liu, J., Venkataraman, G., Rosenberg, R., and Sasisekharan, R. (2002) Expression in *Escherichia coli*, purification and kinetic characterization of human heparan sulfate 3-O-sulfotransferase-1, *Biochem. Biophys. Res. Commun.* 290, 1206–1213.
34. Yabe, T., Shukla, D., Spear, P. G., Rosenberg, R. D., Seeberger, P. H., and Shworak, N. W. (2001) Portable sulphotransferase domain determines sequence specificity of heparan sulphate 3-O-sulphotransferases, *Biochem. J.* 359, 235–241.
35. Griffin, C. C., Linhardt, R. J., Van Gorp, C. L., Toida, T., Hileman, R. E., Schubert, R. L., and Brown, S. E. (1995) Isolation and characterization of heparan sulfate from crude porcine intestinal mucosa peptidoglycan heparin, *Carbohydr. Res.* 276, 183–197.

BI052403N